

NUMERICAL SIMULATION AND VALIDATION OF INTAKE SYSTEMS WITH CFD METHODOLOGY

Luis G. Castillo¹, Jose M. Carrillo¹

¹Department of Civil Engineering, Universidad Politecnica de Cartagena, Spain
Paseo Alfonso XIII, 52, 30203 Cartagena, Spain
E-mail: luis.castillo@upct.es, jose.carrillo@upct.es

Abstract

Intake systems generally consist in a rack located in the bottom of the channel, so that the water collected passes down the rack. These structures have been adopted in small mountain rivers with steep slopes and irregular riverbed, with intense sediment transport and flood flow.

Its design is intended to meet two primary objectives: : to derive as much water as it possible with the minimum solids. Nosedá (1956) studied different typologies of racks. The racks were formed with bars with *T* profiles with the wing willing horizontal parallel to the direction of the flow, and *L* profiles with the long side perpendicular to the horizontal direction of flow. The bars used had the same width, but the longitudinal layout was modified to consider different spacing between them.

In each test was measured the flow collected in the rack and the longitudinal profile of the flow in the centerline of the channel.

The methodology of Computational Fluid Dynamics (*CFD*) simulate the interaction between different fluids, such as the sediment-water two-phase flows that appear in the phenomenon of intake systems.

The methods used in *CFD* are based on numerical solution of the Reynolds Averaged Navier-Stokes (*RANS*) equations, together with turbulence models of different degrees of complexity.

This paper compares some of the experimental results in clear water, obtained by Nosedá with the simulations results obtained with the *CFD* commercial programs *ANSYS CFX* and *FLOW 3D*.

Introduction

When we design a intake system we need considerer aspects geomorphologic, hydraulic, structural and economic in order to avoid unnecessary maintenance and functionality problems during the entire life of the project.

The efficiency of racks depend on diverse factors as e.g. number of bars, flow entrain conditions, inclination, shape and spacing between bars.

The theoretical analysis supposes that the flux over the rack can be treated as a one-dimensional movement with flow progressively decreasing. In this way, it is considered a hydrostatic pressure distribution over the rack in the flow direction.

The hydraulic comportment of the racks is also influenced by the bars disposition. In the longitudinal bars, the flow collected appears as a function of the local energy flow while in transversal bars or circular perforations the flow collected is related with the local flow level (Mostkow, 1957).

Starting form velocity measurements in the free surface, Brunella et al. (2003) obtained that the dissipation effects are insignificant. However, in the final part of the racks this effects cannot be neglected due to the local effects of the flow level generate friction effects.

Righetti et al. (2000) consider that it is possible calculate the flow differential of the water collected with the following formulae:

$$dq(x) = C_q \omega \sqrt{2g(H_0 + \Delta z)} dx \quad (1)$$

where ω is the total area of the spacing, dx is the increment longitudinal in the flow direction, H_0 is the specific energy in the start of the rack, Δz is the difference between the initial rack section and the analyzed section and C_q is the discharge coefficient. According this author, $C_q = \sin \alpha$, being α the angle of the velocity vector of water collected with the rack plane (Figure 1).

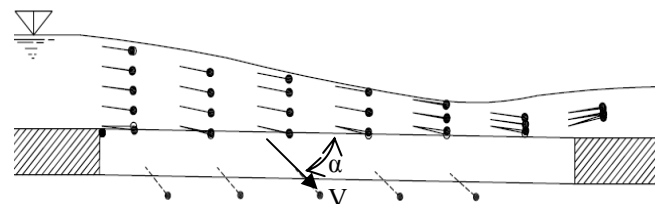


Figure 1: Inclination α of the streamlines of the flow collected, (Righetti et al., 2000)

Purpose

As a result of the existence of boundary layer separations and high turbulence that difficult the study with traditional methodologies, we consider necessary carry out a parallel numerical modeling study in order to complement the data obtained in physics models. For this reason, we used two Computational Fluid Dynamic program (*CFD*) in order to obtain the next points:

- To verify the *ANSYS CFX* and *FLOW 3D* program capacity as a tool of flow analysis over intake systems.
- To prove the accuracy of their solutions, a comparison with the experimental measurements obtained by Nosedá (1956), is carried out.

Physic Model

The physic model studied by Nosedá (Figure 2) was built with Plexiglas wall that permitted to see the flow. It consisted in a 8-meter length and 0.50-meter width channel, a rack with different slopes, the discharge channel and the discharge water collected channel. The rack had aluminum bars and was located in the bottom of the channel.

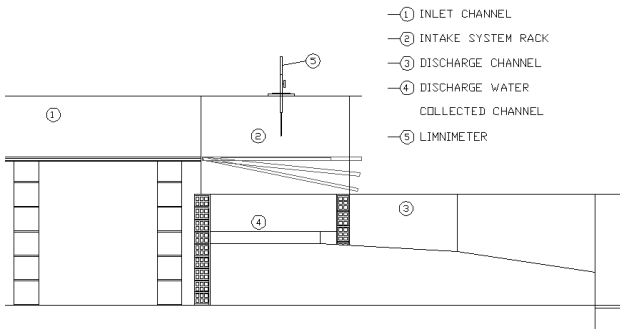


Figure 2: Lab model of the intake system

The experiments were carry out with different types of rack. The racks were built with *T* profile and *L* profile bars. The bars used had the same width, but the longitudinal layout was modified to consider different spacing between them. In Table 1 we can see the geometric characteristics of each experiment that we have modeled with *CFD* program.

Table 1: Geometric characteristics of the lab experiments

Experiment	A	B	C
Length, L (m)	0.900	0.900	0.900
Bar type (mm)	T 30/25/2	T 30/25/2	T 30/25/2
Direction of the flow	Longitudinal	Longitudinal	Longitudinal
Spacing, b_1 (mm)	5.70	8.50	11.70
Coefficient $m = \frac{b_1}{b_1+30}$	0.16	0.22	0.28

In each experiment, the entrain and exit flows and the longitudinal flow profile were measured. q_1 is the entrain specific flow, q_2 is the specific discharge flow and q_d is the specific discharge flow collected in the intake system. Table 2 shows the entrain specific flows measured.

Table 2: Entrain specific flows in the physic model

Nº experiment	1	2	3	4	5
q_1 (l/s/m)	53.8	77.0	114.6	155.4	198.3

Finally, in Table 3 we can see the flow characteristics in the inlet of the intake system where e_0 is the flow specific energy and h_1 is the depth.

Table 3: Principal characteristics in the physic model

Rack type	q_1 (l/s/m)	e_0 (cm)	h_1 (cm)	$\frac{h_1}{e_0}$
Horizontal A, B, C rack with subcritical flow in the inlet	53.8	9.98	6.66	0.667
	77.0	12.68	8.45	0.667
	114.6	16.53	11.02	0.667
	155.6	20.25	13.50	0.667
	198.3	23.82	15.88	0.667

Numerical Model

The Computational Fluid Dynamics programs allow us to simulate the interaction among different fluids as a two-phase air-water or flows and different concentrations in the case of sediment transport. The programs solve the fluid mechanic problem into whatever geometric configuration, providing lot of data, increased profitability, flexibility and speed than that obtained with experimental procedures. However, to a correct use, it is necessary to contrast and to calibrate with data obtained in prototype or physics model. To test the hydraulic compartment of a intake system, the experimental data measured by Nosedá was used in order to model and calibrate the *CFD* program (*ANSYS CFX* and *FLOW 3D*).

The *CFD* codes solve the differential Navier-Stokes equations of the phenomenon in control volumes defined by the meshing of the fluid domain, retaining the reference quantity (mass, momentum, energy) in the three directions for each control volume identified. The Navier-Stokes equations are:

Continuity equation:

$$\frac{\partial \rho}{\partial t} + \nabla \cdot (\rho U) = 0 \quad (2)$$

Momentum equation:

$$\frac{\partial (\rho U)}{\partial t} + \nabla \cdot (\rho U \otimes U) = -\nabla p + \nabla \cdot \tau + S_M \quad (3)$$

Energy equation:

$$\frac{\partial (\rho h_{tot})}{\partial t} - \frac{\partial p}{\partial t} + \nabla \cdot (\rho U h_{tot}) = \nabla \cdot (\lambda \nabla T) + \nabla \cdot (U \cdot \tau) + U \cdot S_M + S_E \quad (4)$$

were

$$\tau = \mu \left(\nabla U + (\nabla U)^T - \frac{2}{3} \delta \nabla \cdot U \right) \quad (5)$$

$$h_{\text{tot}} = h + \frac{1}{2} U^2 \quad (6)$$

being p the pressure, ρ the flow density, U the velocity vector, τ the stress, h the energy, S_M the sum of body forces, S_E the momentum source, λ the volumetric viscosity, μ the dynamic viscosity and δ the Kronecker Delta function.

To complement the numerical solution of Reynolds equations and average Navier-Stokes (*RANS*), has been used turbulence model. There are many turbulent models of diverse complexity, from the isotropic models of two-equation like the classic $k-\epsilon$ to the second moment closure models (*SMC*) like the Reynolds Stress Model.

The *SMC* models are based on the solution of a transport equation for each of the independent Reynolds stresses in combination with the $k-\epsilon$ or the $k-\omega$ equation. The experience shows that the increased number of transport equations in the *SMC* models leads to reduced numerical robustness, requires increased computational effort and for this reason are rarely used.

The two-equation models has been widely applied in the solution of many flows of engineering interest. The $k-\epsilon$ (*k-epsilon*) model, has been implemented in most general purpose *CFD* codes and is considered the industry standard model, but may not be suitable to solve flows with boundary layer separation. The $k-\omega$ based models try to give a highly accurate predictions of the flow separation.

In *ANSYS CFX* we used the $k-\omega$ based Shear-Stress-Transport (*SST*) model. This model was designed to give a highly accurate predictions of the onset and the amount of flow separation under adverse pressure gradients by the inclusion of transport effects into the formulation of the eddy-viscosity. The best performance of this model has been demonstrated in a large number of validation studies (Bardina et al, 1997).

In *FLOW 3D* we used the Renormalization-Group (*RNG*) $k-\epsilon$ model (Yakhot and Orszag, 1986; Yakhot and Smith, 1992). This turbulence model applies statistical methods to the derivation of the averaged equations for turbulence quantities, such as turbulent kinetic energy and its dissipation rate. Generally, the *RNG* $k-\epsilon$ model has wider applicability than the standard $k-\epsilon$ model. In particular, the *RNG* model is known to describe low intensity turbulence flows and flows having strong shear regions more accurately (Flow 3D, 2011).

To solve the two-phase air-water in *ANSYS CFX* we used the homogeneous model. In *FLOW 3D* we selected the one fluid option, join the air entrainment models.

In the study of intake system exist flow separation and high turbulence that need high quality mesh elements in order to solve the problem with the highest accuracy.

We have used in both program hexahedral mesh elements. The total number of elements used in the *ANSYS CFX* simulation was 109,262 elements, with 0.004 m length scale near the rack and 0.008 m in the rest of the model. In *FLOW 3D* we used mesh size with 0.002 m length scale near the rack and 0.004 m in the rest of the model in order to approach to the bar contours, using 331,484 elements.

The model boundary conditions corresponds to the flow at the inlet, upstream and downstream levels and their hydrostatic pressures distributions. In the bottom of the exit channel of water collected by the rack we used opening boundary condition in *ANSYS CFX* and outflow in *FLOW 3D* due that in this boundary the hydrostatic pressure condition is not allow.

For simplicity, we considered that in the intake system all the longitudinal bars work in the same mode. For this reason, we considered the existence of symmetry conditions in the central plane of the spacing between bars. In Figure 3 we can see that the domain fluid modeled have the longitudinal bar in the middle of two symmetry conditions.

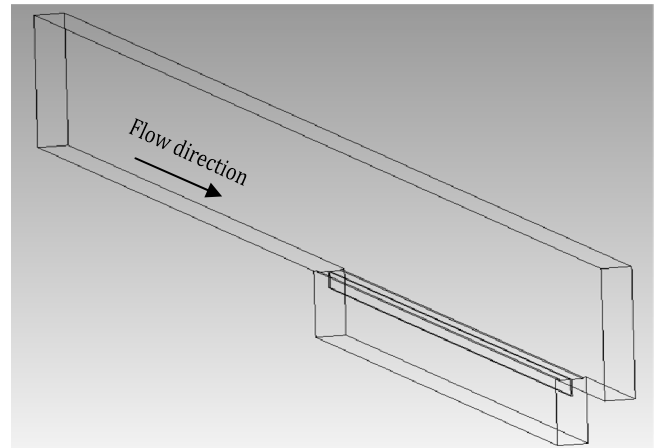


Figure 3: Detail of fluid domain geometry

ANSYS CFX allows to model steady state simulations. We have used a 0.05-second time-step. Using a 8-core CPU, the mean resolution time was 1.20 hours.

In *FLOW 3D* it is only able to run transient state simulations. However it is possible to use stop criteria when the simulation reach the steady state. The timescale is obtained in each step in order to satisfy different internal stability criteria. Figure 4 shows the evolution of the time-step size in each step and how the time-step decreases when the simulation is reaching the steady state. The final time-step in the majority of the simulations was near 0.0002 seconds, requiring 1.30 hours to solve the whole problem. However, in some simulations the time-step reached the 0.00002 seconds, increasing the time resolution up to 11 hours.

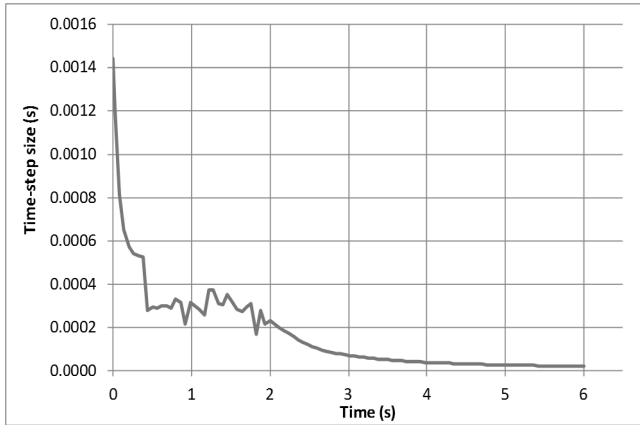


Figure 4: Varying of the time-step size in *FLOW 3D*.

Results and Discussion

In order to know the accuracy of the numerical simulations data, in the first place, we are going to compare the longitudinal flow profiles over the centre of the bar with the results obtained in the physic model by Nosedá.

Figure 5 compares the flow profiles measured in lab over the centre of the bars with the data obtained with the two programs, with spacing $b_l = 11.70$ mm (coefficient $m=0.28$) and specific flow $q_l = 198.30$ l/s/m and $q_l = 53.80$ l/s/m. We can see that, for the biggest spacing between bars, the water profiles obtained with *CDF* methodology are very similar to the lab measurements.

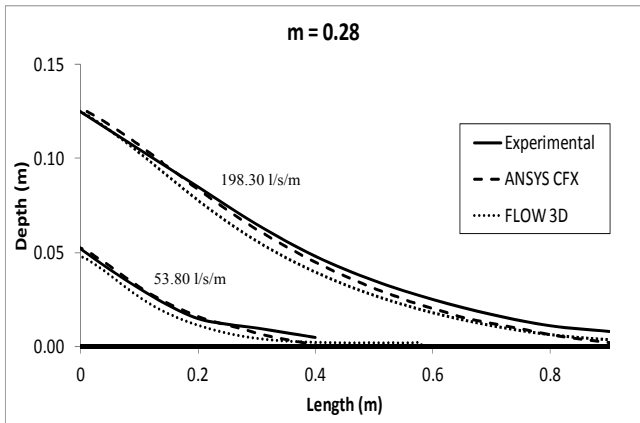


Figure 5: Flow profiles over the centre of the bar with horizontal rack, $b_l = 11.70$ mm and q_l 53.8 and 198.30 l/s/m

In a similar way, Figure 6 compares the depth of the longitudinal flow profiles obtained with the biggest and the smallest specific flows using the three methodologies, and considering spacing $b_l = 8.50$ mm ($m = 0.22$) and specific flow $q_l = 198.30$ l/s/m and $q_l = 53.80$ l/s/m. We can see that *ANSYS CFX* obtains a profile a little more accurate than *FLOW 3D*.

Finally, Figure 7 graphs the depth water profiles considering $b_l = 5.70$ mm ($m = 0.16$) and specific flow $q_l = 198.30$ l/s/m and $q_l = 53.80$ l/s/m. We can observe that *ANSYS CFX* reproduces with better accuracy the free

surface profiles, while *FLOW 3D* obtains profiles up to 1.5 cm below the lab measurements in the final part of the rack.

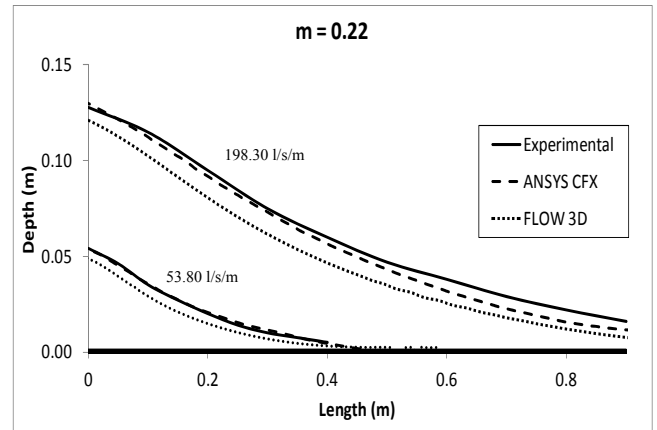


Figure 6: Flow profiles over the centre of the bar with horizontal rack, $b_l = 8.50$ mm and q_l 53.8 and 198.30 l/s/m

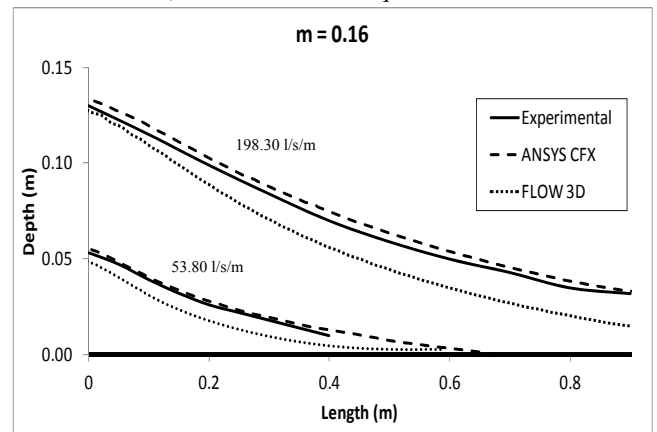


Figure 7: Flow profiles over the centre of the bar with horizontal rack, $b_l = 5.70$ mm and q_l 53.8 and 198.30 l/s/m

After this, we compare the ratio between specific flow, q_l , and specific flow collected in the intake system, q_{di} , for the three spacing.

In this way, in Figure 8 we can see that the ratio flow entrain-flow collected is almost the same for the intake system with the biggest separation between bars.

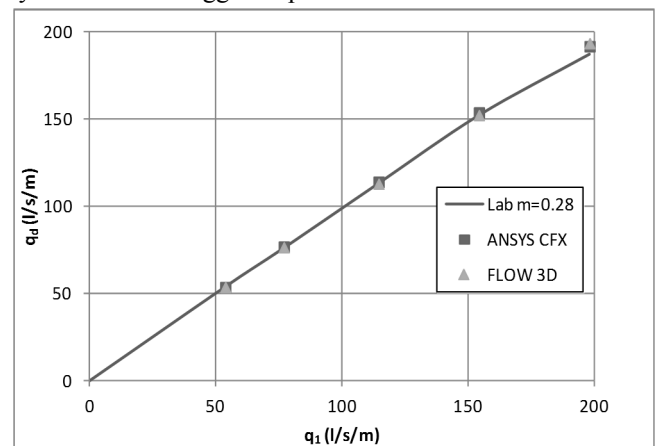


Figure 8: Derivation capacity of the intake system, with $b_l = 11.70$ mm

With the intermedium spacing, we obtained similar results too, except for $q_I=198.31\text{ l/s/m}$ in which both programs collect more flow (Figure 9).

The results obtained in the modelation of the highest flow rates with the smallest separation (Figure 10) shows that FLOW 3D collects more flow than the lab measurements.

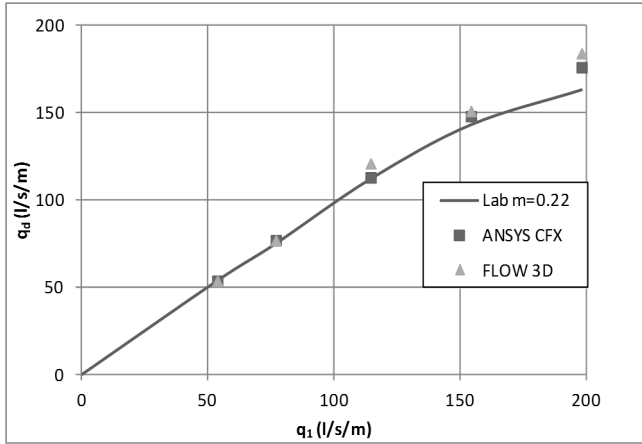


Figure 9: Derivation capacity of the intake system, with $b_I=8.50\text{ mm}$

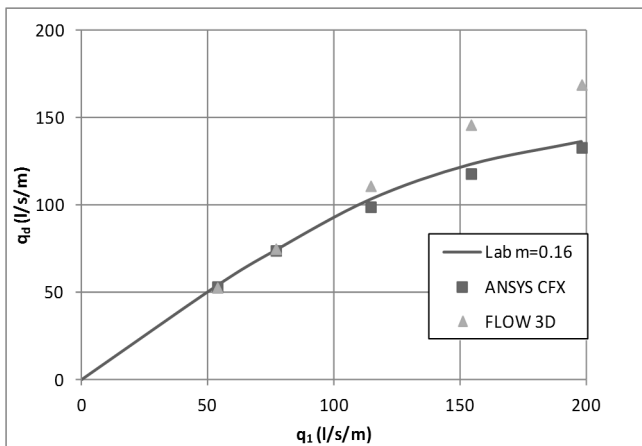


Figure 10: Derivation capacity of the intake system, with $b_I=5.70\text{ mm}$

Carrying out a qualitative analysis of streamlines, in Figure 11 and 12 we can see the semejance among the streamlines calculated in the numeric simulations and the obtained with laser methodology by Righetti and Lanzoni (2008).

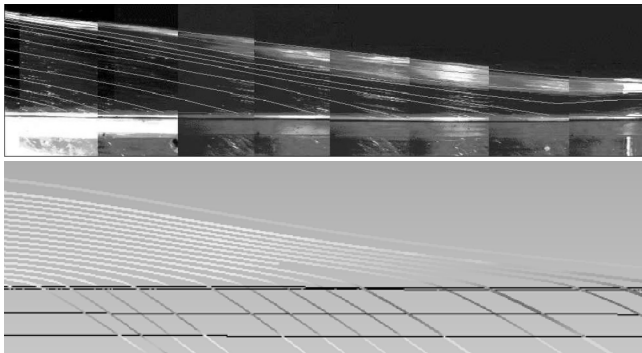


Figure 11: Streamlines over the rack. Up: Photo with laser light by Righetti and Lanzoni (2008). Down: Result obtained with ANSYS CFX

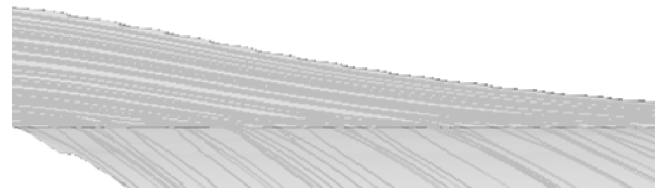


Figure 12: Streamlines over the rack. Result obtained with FLOW 3D

Finally, we compare the angle of the velocity vector of water collected with the rack plane, α , measured in the centre of the spacing between bars.

Righetti et al. (2000) obtained in their lab studies that the range of $\sin \alpha$ is among 0.5 and 0.7, reducing according the depth water decrease.

Figures 13, 14 and 15 shows the results obtained with numerical simulations using CFD programs for the specific flow $q_I=198.30\text{ l/s/m}$ and $q_I=53.80\text{ l/s/m}$. Despite the fact that we have used different setting bars and flows, we can see that the values obtained are in the same rate than the observed in lab, reducing $\sin \alpha$ downstream with the decreasing of the depth water, where the result obtained with FLOW 3D show a little more variability of $\sin \alpha$.

On the other hand, there are not significant variations among the results obtained with different spacing.

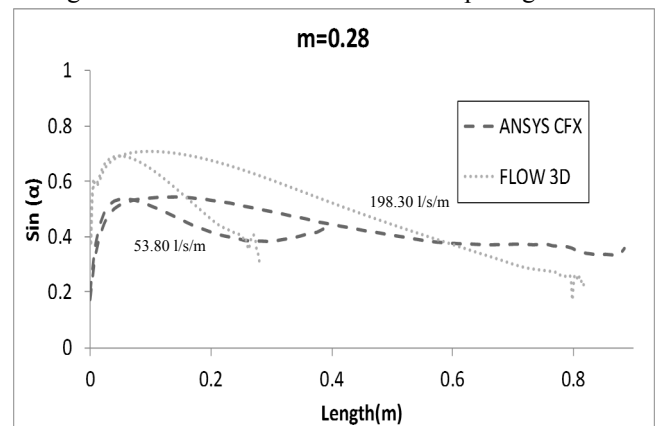


Figure 13: Variation of $\sin(\alpha)$ in the centre of the spacing, with $b_I=11.70\text{ mm}$ and $q_I 53.8$ and 198.30 l/s/m

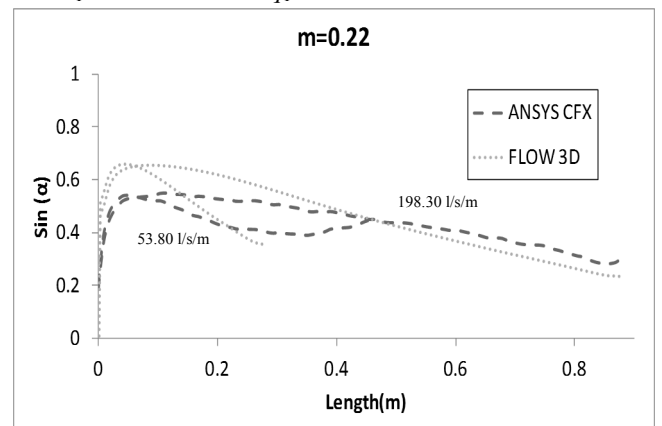


Figure 14: Variation of $\sin(\alpha)$ in the centre of the spacing, with $b_I=8.50\text{ mm}$ and $q_I 53.8$ and 198.30 l/s/m

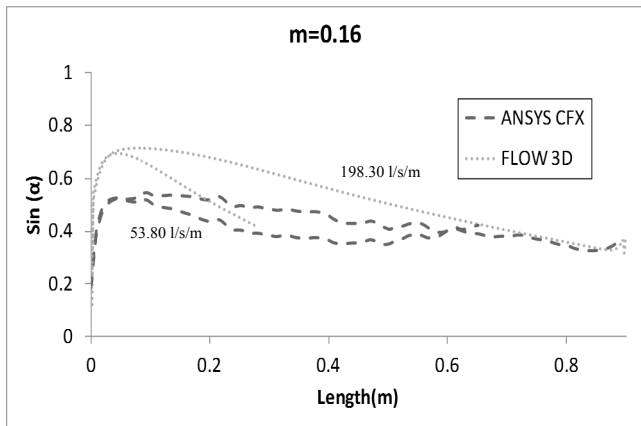


Figure 15: Variation of $\sin(\alpha)$ in the centre of the spacing, with $b_1 = 5.70$ mm and q_1 53.8 and 198.30 l/s/m

Conclusions

In this paper we have tested the accuracy of the numeric results obtained with *CFD* methodology in order to model a intake system.

With these results, we can highlight the following advantages of each program in the intake system modeling:

ANSYS CFX

- Allows to use a steady state.
- We can use a fix time-step so that we approximately know when the simulation will finish.
- $k-\omega$ based and second moment closure turbulence models can be used.

FLOW 3D

- We can verify the evolution of the solution while it is solving the problem.
- It is possible to use a stop criteria when the steady state is reached.
- The water free surface obtaining is easier.

In summary, we can say that *ANSYS CFX* has a little more capacity to model flows over intake systems.

Nevertheless, to improve knowledge in this area it is necessary to make more experimental studies, both physical models and prototypes, simultaneously characterizing the phenomena produced over the rack and measured of depths, velocities and sediment rates. This will allow us to calibrate and validate the *CFD* codes.

Future Works

This work consists in the study of clean water over a rack using *CFD* methodology. In order to improve the knowledge of this structures, we are building an intake system in the Hydraulic Laboratory of the Universidad Politecnica de Cartagena (Figure 16).

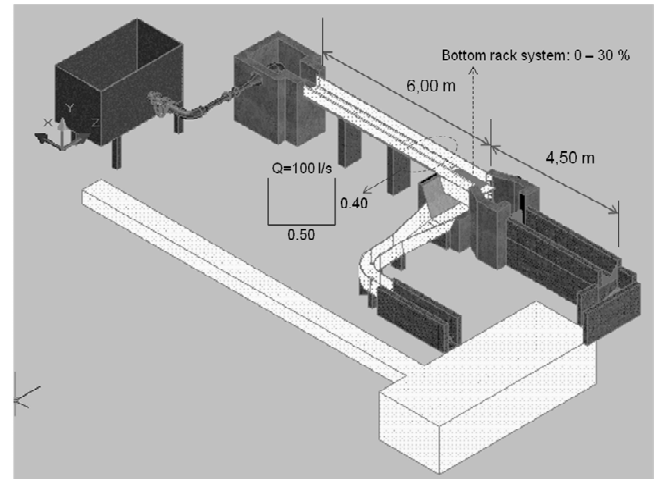


Figure 16: Physic model of intake system

We will analyze different configuration of bars (shape, spacing, tilt) and the effect of different sediment concentrations flowing over a intake system.

Acknowledgments

The research is part of the project PEPLAN: "Hydrological modeling in Semi-Arid Regions. Subproject 3: Modeling of intakes in ephemeral rivers". The authors are grateful for financial support of Consejería de Universidades, Empresa e Investigación of Comunidad Autónoma of Región de Murcia.

References

- ANSYS CFX (2010). ANSYS, Inc. ANSYS CFX. Reference Guide. Release 13.0.
- Bardina, J.E., Huang, P.G. & Coakley, T.J. (1997). Turbulence Modeling Validation Testing and Development. *NASA Technical Memorandum* 110446.
- Brunella, S., Hager, W. & Minor, H. (2003). Hydraulics of Bottom Rack Intake. *Journal of Hydraulic Engineering*/ January, USA: 4- 9.
- Castillo, L. & Lima, P. (2010). Análisis del dimensionamiento de la longitud de reja en una captación de fondo. *XXIV Congreso Latinoamericano de Hidráulica*, Punta del Este, Uruguay.
- FLOW 3D (2011). FLOW Science, Inc. *FLOW 3D. Theory v10.0*.
- Noseda, G. (1956). Correnti permanenti con portata progressivamente decrescente, defluenti su griglie di fondo. *L'Energia Elettrica*, pp. 565-581.
- Righetti, M., Rigon, R. & Lanzoni, S. (2000). Indagine sperimentale del deflusso attraverso una griglia di fondo a barre longitudinali. *Proc., XXVII Convegno di Idraulica e Costruzioni Idrauliche*, Vol. 3, Genova, Italy, 112-119.
- Righetti, M. & Lanzoni, S. (2008). Experimental Study of the Flow Field over Bottom Intake Racks. *Journal of Hydraulic Engineering © ASCE/ January 2008/pp. 15-22*.
- Yakhot, V. & Orszag, S.A. (1986). Renormalization group analysis of turbulence. I. Basic theory. *Journal of Scientific Computing*, Volume 1, Number 1, pp. 3-51.
- Yakhot, V. & Smith, L.M. (1992). The renormalization group, the ϵ -expansion and derivation of turbulence models. *Journal of Scientific Computing*, Volume 7, Number 1, pp. 1.